J Electr Eng Technol.2015; 10(4): 1786-1795
http://dx.doi.org/10.5370/JEET.2015.10.4.1786

ISSN(Print) 1975-0102
ISSN(Online) 2093-7423

Experimence Study of Trace Water and Oxygen Impact on SF_6 Decomposition Characteristics Under Partial Discharge

Fuping Zeng*, Ju Tang†, Yanbin Xie, Qian Zhou*** and Chaohai Zhang§**

Abstract – It is common practice to identify the insulation faults of GIS through monitor the contents of SF_6 decomposed components. Partial discharges (PD) could lead to the decomposition of SF_6 dielectric, so new reactions usually occur in the mixture of the newly decomposed components including traces of H_2O and O_2. The new reactions also cause the decomposed components to differ due to the different amounts of H_2O and O_2 even under the same strength of PD. Thus, the accuracy of assessing the insulation faults is definitely influenced when using the concentration and corresponding change of decomposed components. In the present research, a needle-plate electrode was employed to simulate the PD event of a metal protrusion insulation fault for two main characteristic components SO_2F_2 and SOF_2, and to carry out influence analysis of trace H_2O and O_2 on the characteristic components. The research shows that trace H_2O has the capability of catching an F atom, which inhibits low-sulfide SF_x from recombining into high-sulfide SF_6. Thus, the amount of SOF_2 strongly correlates to the amount of trace H_2O, whereas the amount of SO_2F_2 is weakly related to trace H_2O. Furthermore, the dilution effect of trace O_2 on SOF_2 obviously exceeds that of SO_2F_2.

Keywords: Partial discharge, SF_6, Decomposed component concentration, Trace H_2O and O_2, Influence regularity

1. Introduction

Different patterns and strengths of partial discharge (PD) always occur when SF_6 electrical equipment have some earlier insulation faults. High local electromagnetic energy caused by PD would cause SF_6 to decompose into several kinds of low-fluoride sulfide SF_x [1-4]. If trace levels of H_2O and O_2 exist in the equipment, the decomposed components would have further reactions with them and produce new characteristic components, such as SO_2F_2, SOF_2, SO_2, and so on [5-11]. The concentration and variation regularity of these characteristic components have close relationship with the patterns of insulation faults, as well as the trace levels of H_2O and O_2 in gaseous SF_6, making it more difficult to recognize the internal insulation deficiency when using them. Although the new gas SF_6 contains few impurities, trace levels of H_2O and O_2 would enter the gas chamber as they are released from internal material or by penetration from the outside air over time [12]. There would be extra-trace levels of H_2O and O_2 inevitably existing in the SF_6 electrical equipment. Hence, when extra-trace levels of H_2O and O_2 exist in SF_6 gas, learning about the decomposition mechanism from both theory and experiment under PD are necessary; obtaining the influence regularity and influence mechanism of trace H_2O and O_2 on decomposed components is urgent. Furthermore, it is imperative to offer a amendment method considering the impacts of trace H_2O and O_2 so that all of the aforementioned methods would lay a solid theoretical foundation for the correct identification and evaluation of the internal insulation faults of SF_6 electrical equipment when making use of the decomposed components.

R. J. Van Brunt from the U.S. National Bureau of Standards conducted a systematic research about the SF_6 decomposition mechanism under PD. He studied the main source [13] of the O atom in SO_2F_2, SOF_2, and SOF_4 using the isotopic tracer technique under the condition of needle-plate electrode of corona discharge. His study pointed out that the O atom of SO_2F_2 mainly comes from O_2, the O atom of SOF_2 mainly comes from H_2O, and the O atom of SOF_4 comes from both O_2 and H_2O. However, the paper also claimed that SO_2F_2 obtains the O atom from H_2O and SOF_2 obtains the O atom from O_2. Nevertheless, the Van Brunt research used the same fixed concentration of H_2O and O_2 without considering their levels of variation. According to Arrhenius' law of chemical reaction kinetics and mass action law [14], the chemical reaction rate depends on the reaction temperature, reactant concentration, and catalyst. Although Derdouri studied the impact of diverse concentrations of H_2O on SF_6 gas under PD, there is a lack of explanation of the process [15].

† Corresponding Author: School of Electrical Engineering, Wuhan University, China. (whtangju@whu.edu.cn)
* School of Electrical Engineering, Wuhan University, China. (Fuping.Zeng@whu.edu.cn)
** State Grid Chongqing Electric Power Company, Shiqu Power Supply Company, China. (yanbinse@126.com)
*** State Grid Chongqing Electric Power Company, China. (cquzhou@163.com)
§ Wuhan NARI Limited Company of State Grid Electric Power Research Institute, China. (zhangchaohai@sgepri.sgcc.com.cn)
Received: October 5, 2014; Accepted: March 31, 2015

In this paper, the authors take advantage of the PD decomposition platform in the laboratory and study the concentration of decomposed SF_6 components and their variation trends under PD when different trace levels of H_2O and O_2 are mixed with SF_6. Moreover, the mechanism of how the various concentrations of trace water and oxygen act on the characteristic decomposed components from the angle of related chemical reaction rate is explained. Considering that random factors may lead to unfavorable results during the experiment, statistical inference using ANOVA is used to investigate the degree of impact of trace H_2O and O_2 on decomposed characteristic components of SF_6.

2. Decomposition Experiment and Quantitative Measurement

2.1 Experiment

This work studies the degree of influence of H_2O and O_2 on decomposed characteristic components of SF_6 under PD from the statistical perspective. Hence, repeating the experiment independently n (here n=4) times under the same trace levels of H_2O and O_2 (the level is A_i) and making sure that each experiment group has only one variable. The procedure suggests that the concentration of O_2 is controlled below 100ppm (the rate of oxygen analyzer is 100ppm) in the experiment gas sample when the experiment on the influence of different trace levels of H_2O was conducted. Likewise, the concentration of H_2O is controlled below 150 ppm when the experiment on the influence of different trace levels of O_2 was conducted. Experimental factors A (H_2O) and B (O_2) were subjected into seven experimental levels, as shown in Table 1.

Experiment material: SF_6 (purity: 99.99%, $H_2O \leq 100$ ppm, $O_2 \leq 100$ppm), H_2O, and O_2 were used as experiment materials. The experiment was conducted in the multi-function electrical decomposition of SF_6 equipment designed by our group, which is shown in Fig. 1 [16]. The main body of gas chamber is cylinder and both ends are oval structure to guarantee its air tightness. The volume of the chamber is approximately 10L and the maximum tolerance of air pressure can reach 0.5Mpa. The material of gas chamber is made of stainless steel for its corrosion resistance since the corrosive decomposed compositions of

Table 1. Factors affecting the by-product yields

Level	A (H_2O) in ppm		B (O_2) in ppm	
1	300		100	
2	700		220	
3	1000		460	
4	1300	O_2 < 100ppm	900	H_2O <150ppm
5	1600		2140	
6	1800		4960	
7	2100		10250	

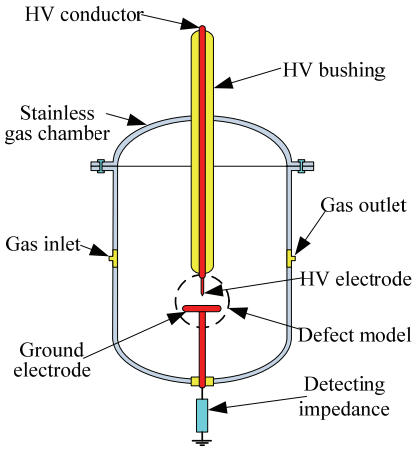

Fig. 1. SF_6 decomposition gas chamber

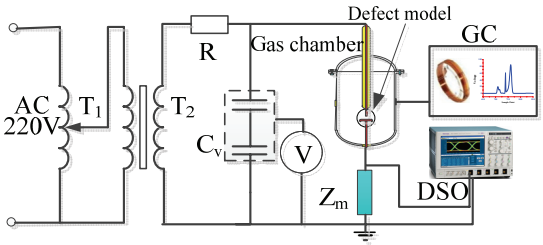

Fig. 2. Experimental system diagram

SF_6 may be produced during the experiment. Lead the HV conductor in the gas chamber through HV bushing and the model of insulation faults is positioned in the middle of the gas chamber so that it can connect with bottle of the HV conductor. Gas inlet and gas outlet is equipped to fill in SF_6 required in the experiment and gather the mixed gases sample after PD experiment.

The gas chamber was filled with 0.2 MPa of SF_6. The experimental system diagram is shown in Fig. 2. The needle-plate electrode is needed to simulate the common insulation fault (metal protrusion insulation fault) in the equipment. Moreover, the experiment made use of non-inductive detected impedance to send the pulse current signal to the WavePro 7100XL oscilloscope (Analog band: 1 GHz; sampling rate: 20 GHz; memory depth: 48 MB), which can monitor whether the PD is stable.

2.2 Experiment methods

This experiment uses needle-plate electrode model: spacing d is 10mm, curvature radius of needle tip is 0.3mm, diameter of ground electrode is 120mm and its thickness is 10mm. All the experiments are conducted at the same condition: the laboratory temperature is controlled at 15℃ and relative humility at 50%, to avoid the impacts of different temperatures and humidity and ensure the experimental results are comparable. The specific experimental requisition and steps are listed as follows:

(1) Measurement of the initial voltage U_s of the intrinsic

PD of the equipment (without putting insulation faults model) and the initial voltage U_0 of the PD of the equipment (after putting the needle-plate electrodes). The respective measurements are U_s=45 kV and U_0= 15 kV.

(2) The gas chamber is vacuumized and then filled with new gas, SF_6, and vacuumized again. This process is repeated two or three times for purification.

(3) For the experimental procedure on the influence of H_2O on the decomposed characteristic components of SF_6, step (4) is used. Otherwise, for the experiment on the influence of O_2 on the decomposed characteristic components of SF_6, step (5) is used.

(4) The gas chamber is filled with the required amount of H_2O by gas-syringe when the chamber is in vacuum condition, and subsequently heated in the equipment for 15 minutes. Another 15 minutes is spent to permit the H_2O to undergo gasification and uniform distribution in the gas chamber. Step (6) follows.

(5) The gas chamber is filled with the required amount of O_2 when the chamber is in vacuum condition. Another 15 minutes is spent to permit the full volume of O_2 to be uniformly distributed in the chamber.

(6) The gas chamber is filled with SF_6 equivalent to a pressure of 0.25 MPa and put aside for 24 hours, so that H_2O (or O_2) and SF_6 are fully mixed.

(7) The concentration of H_2O and O_2 in the mixed gas is measured. If the concentration fails to meet the experimental standards, the procedure goes back to step (2). When the measured concentrations have satisfied the standards, the gas sample is collected and its intrinsic components are analyzed. The respective concentrations of the constituent gases are also measured. Afterward, the mixed gas pressure is adjusted to 0.2 MPa.

(8) The electrical wiring is connected as shown in Fig. 2. The experimental voltage is then gradually raised to $1.5U_0$ (22.5 kV) and the PD decomposition experiment is conducted for 10 hours under this voltage. This part of the procedure ensures that the contents of the characteristic components are stable. The oscilloscope is used to monitor the electrical discharge of the needle-plate electrode.

(9) After 10 hours, the concentration of the different decomposed components in the collected gas sample is analyzed using gas chromatograph (GC).

(10) After measuring all the experimental parameters, the gas chamber is vacuumized and put aside for 1 hour to enable absorption of the decomposed components by the surface of the electrode. The time allowance is also aimed to fully extricate the decomposed components attached on the chamber wall and inhibit the impact of the remaining components of the on-going experiment to the next experiment. The procedure is then repeated from step (2) for the next experiment.

2.3 Quantitative measurement of decomposed components

In the aforementioned experiments, the gas chromatograph (Varian CP-3800) was used to quantitatively measure the sample gas components produced by the discharge. The GC used the packed column Porapak QS and special capillary column CP-Sil 5 CB in parallel to separate the components in the mixture. Moreover, the chromatograph used PDHID double detectors (detection precision can reach up to 0.01ppm) to quantitatively detect each separated component. The chromatographic column was operated in the He (purity: 99.999%) carrier gas and the working conditions were flow rate, 2 mL/min; constant column

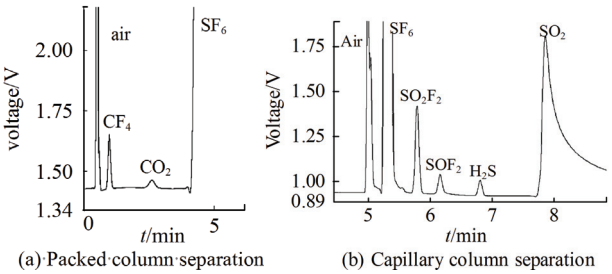

Fig. 3. Standard chromatogram

Table 2. The raw data of each experiment (ppm)

Trace-H_2O	SO_2F_2				
	300	13.43	14.13	10.52	11.42
	700	14.11	13.32	15.56	14.01
	1000	13.8	14.21	16.03	14.87
	1300	15.48	16.91	11.48	12.06
	1600	15.16	15.28	12.25	14.69
	1800	18.66	15.33	16.25	17.72
	2100	19.78	15.11	14.3	14.68
	SOF_2				
	300	32.66	30.66	25.64	30.01
	700	38.93	39.68	41.38	39.83
	1000	42.57	40.25	46.68	38.54
	1300	46.9	52.64	48.01	48.43
	1600	51.35	49.22	50.98	54.44
	1800	61.88	55.91	54.71	58.89
	2100	68.48	65.32	66.78	64.53
Trace-O_2	SO_2F_2				
	100	13.43	14.13	10.52	11.42
	220	5.99	4.92	7.26	7.13
	460	5.51	7.53	7	3.31
	900	5.31	8.99	4.63	5.72
	2140	8.69	9.98	4.87	5.79
	4960	7.78	7.04	7.03	8.93
	10250	15.62	4.87	14.36	9.54
	SOF_2				
	100	32.66	30.66	25.64	30.01
	220	19.05	13.97	18.1	18.95
	460	14.09	14.28	15.71	11.66
	900	13.85	18.22	11.78	12.38
	2140	15.82	16.81	10.99	11.2
	4960	12.07	12.36	12.36	14.03
	10250	26.85	10.99	14.95	16.09

temperature, 40 °C; sample size, 1 mL; and split ratio, 10:1. Under these conditions, the packed column could separate air, CF_4, and CO_2 effectively, and the special capillary column could separate air, SF_6, SO_2F_2, SOF_2, H_2S, and SO_2 effectively. Fig. 3 shows the standard chromatograph.

This study used the external standard method combined with the standard chromatogram to qualitatively and quantitatively detect the decomposed components of SF_6. Since the SO_2F_2 and SOF_2 are the most important characteristic decomposed components of SF_6 [1, 3, 6-8, 13, 17, 18], the present study conducted intensive research on both. The raw data of each experiment as show in Table 2, Figs. 4 and 5 are the results of production amounts of the SO_2F_2 and SOF_2 yields under PD at different levels of H_2O and O_2 in 10 hours (Each result is the production average value of four times repeated experiments under the same level of trace H_2O or O_2).

3. Influence of H_2O and O_2 on Characteristic Components

Fig. 4 and Fig. 5 show that different levels of H_2O and O_2 contribute to different concentrations of SO_2F_2 and SOF_2 produced by SF_6 even under the same strength and time length of PD. Besides, the inevitable random factors which exert impacts on the experiment results should be considered in the experiment. Hence, the authors used ANOVA to study the impact of the various levels of trace H_2O and O_2 on characteristic components SO_2F_2 and SOF_2 and indentify the main influence factors on the production of SO_2F_2 and SOF_2.

3.1 Analysis of variance

ANOVA was introduced by the American statistician Fisher in an agricultural experiment [19]. Subsequently, the method has been widely used in other areas, especially in data analysis of industrial experiments where the method ANOVA shows that the total variance (S_T^2) in the sample data can be divided into two parts: variance between groups (S_A^2) and variance within groups (S_E^2). S_A^2 is caused by controllable influential factors of different levels and S_E^2 is caused by all random errors, that is $S_T^2 = S_A^2 + S_E^2$. The size of the difference between groups and the size of the difference within groups are compared to identify the degree of impact of each level on the experimental results, where S_T^2, S_A^2, and S_E^2 can be achieved from Equ. (1) to (3):

$$S_T^2 = \sum_{i=1}^{r}\sum_{j=1}^{n}(x_{ij} - \bar{x})^2 \quad (1)$$

$$S_A^2 = n\sum_{i=1}^{r}(\bar{x}_i. - \bar{x})^2 \quad (2)$$

$$S_E^2 = \sum_{i=1}^{r}\sum_{j=1}^{n}(x_{ij} - \bar{x}_{i.})^2 \quad (3)$$

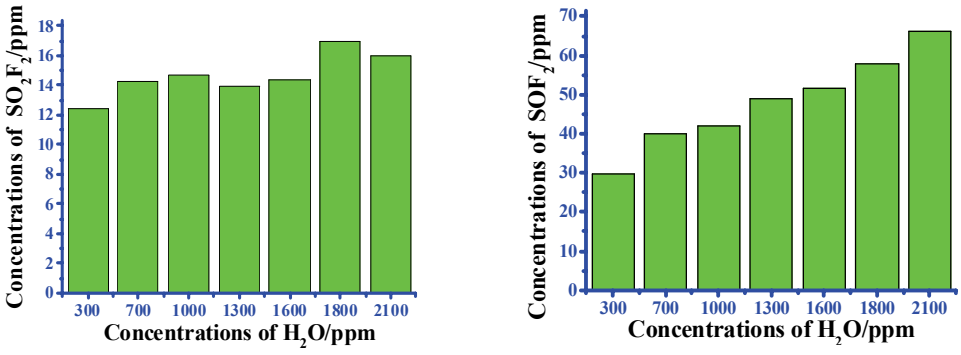

(a) SO_2F_2 (b) SOF_2

Fig. 4. Yield of by-products influenced by H_2O

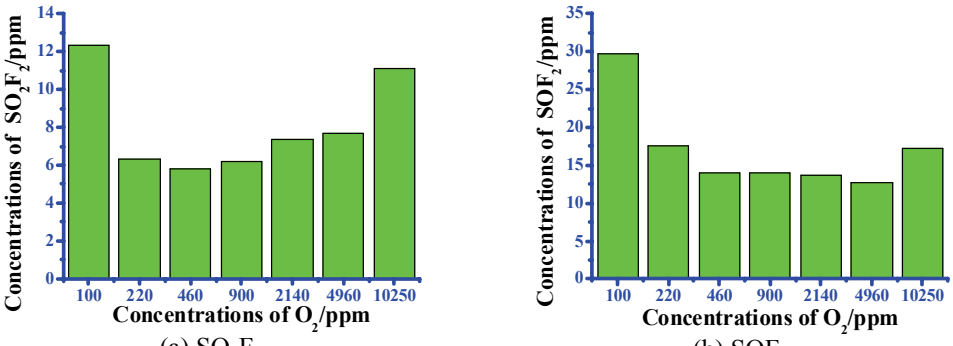

(a) SO_2F_2 (b) SOF_2

Fig. 5. Yield of by-products influenced by O_2

In the above equations, x_{ij} is the *j-th* independent experimental result under the *i-th* concentration level of trace H_2O and O_2 (A_i), which means it is the result of the concentration of SOF_2 or SOF_2 when conducting the *j-th* experiment independently under the *i-th* concentration level of trace H_2O and O_2(A_i); $\overline{x}_i$ represents the group mean of the product of SO_2F_2 or SOF_2 under the *i-th* concentration level of trace H_2O and O_2 (A_i) when conducting experiment *n* times independently; $\overline{x}$ represents the mean of all the products of SO_2F_2 or SOF_2 under the same influence factor (trace H_2O or O_2) in *r* experimental levels; and *r* is the number of influence factor (trace H_2O and O_2) concentration level. There are seven concentration levels in the present study, hence, r =7. n is the number of times the experiment is repeated under the same condition, and in the current study, the experiment is repeated 4 times under the same concentration of trace H_2O and O_2, thus, n =4.

If all the experimental factors (trace H_2O and O_2) have no significant influence in the experimental results, S_A^2 is almost equal to S_E^2 and statistics can prove that

$$F = \frac{S_A^2/(r-1)}{S_E^2/r(n-1)} \sim F(r-1, rn-r) \tag{4}$$

In the equation, $(r-1)$, $r(n-1)$ are the degrees of freedom of S_A^2 and S_E^2, respectively. Furthermore, let $\overline{S}_A^2 = S_A^2/(r-1)$, $\overline{S}_E^2 = S_E^2/r(n-1)$ and call them mean variance, so that equation (4) can be simplified as

$$F = \frac{\overline{S}_A^2}{\overline{S}_E^2} \sim F(r-1, rn-r) \tag{5}$$

ANOVA merely makes use of equation (5) to identify the degree of impact of each level (trace H_2O or O_2) on the experimental results by comparing the differences between groups and the differences within groups. Given the significance level α, when the calculated value of F is above the critical value $F_{1-\alpha}(r-1, rn-r)$, the influence factor (trace H_2O or O_2) has significant influence on the experimental index (generation amount of SO_2F_2 and/or SOF_2). Furthermore, the bigger the F value of the sample, the more significant influence the factor has on the experimental index. Hence, specific attention has to be accorded on such influence factor, and additionally such influence factors should be controlled during practical production.

3.2 Analysis of the significance level of influence factors

Significance level α is a critical probable value that represents the possibility to commit the fallacy of refusing the 'assumption' in a 'statistical hypothesis test' when using the sample information to draw conclusion. The smaller the value of α, the lesser the possibility of making the mistake of refusing the 'assumption'. When analyzing data in the field of general industry, $\alpha = 0.05$; in the field of biology and medicine, $\alpha = 0.01$. In the present study which examines the degree of influence of trace H_2O and O_2 on the main characteristic components of SF_6 (SO_2F_2 and SOF_2) under PD, high precision is required. Hence, a significance level of $\alpha = 0.01$ is adopted. The table of F-distribution critical values shows that $F_{0.99}$ (6, 21) = 3.81. The result is presented in Table 3.

Table 3. Analysis of variance result

Decomposed component	Influence factor	Error	Degree of freedom	Mean variance $\overline{S}_A^2$ or $\overline{S}_E^2$	*Value of F*	Is influence significant?
SO_2F_2	H_2O	S_A^2	6	16.82	3.52	not obvious
		S_E^2	21	4.44		
	O_2	S_A^2	6	26.69	4.44	yes
		S_E^2	21	6.01		
SOF_2	H_2O	S_A^2	6	392.34	87.94	especially
		S_E^2	21	7.26		
	O_2	S_A^2	6	140.03	11.98	especially
		S_E^2	21	11.69		

By collating and analyzing the results from Fig. 4, Fig. 5, and Table 3, the findings indicate that both H_2O and O_2 exert an influence on the main characteristic components SO_2F_2 and SOF_2. However, the products and the degree of influence of H_2O and O_2 are different. The differences include the fact that H_2O has an obvious influence on SOF_2 as the F value reaches 87.94, which is much larger than its influence on SO_2F_2. The formation of SOF_2 is linearly proportional to the concentration of H_2O, but the formation of SO_2F_2 has almost no relationship with the concentration of H_2O. O_2 has a significant effect on both SO_2F_2 and SOF_2, but the impact on SOF_2 is significantly higher than the impact on SO_2F_2.

The existence of H_2O has an effect on the decomposition, as shown by Van Brunt. However, the effect caused by O_2 I is different, which may be due to the fact that Van Brunt did his experiment under the same concentration of O_2 and H_2O without taking into account the concentration of the reactants on the relevant reaction when exploring the sources of O in SOF_2 and SO_2F_2.

4. The influence Mechanism of H_2O and O_2 on the Characteristic Decomposed Components

Under PD, a series of characteristic components are produced by the reaction between the low-fluoride sulfide caused by the decomposition of SF_6 and the trace levels of H_2O and O_2 mixed in the gas. Van Brunt carried out a more detailed study of the SF_6 decomposition mechanism under

PD with a needle-plate electrode mode. He proposed using the Plasma Chemical Model to explain the SF_6 decomposition mechanism under PD [8]. He pointed out that under the effect of the high-energy electrons generated by the PD, the following reaction will occur in SF_6:

$$e + SF_6 \rightarrow SF_X + (6 - x)F + e,\ x = 1 \sim 5 \tag{6}$$

The high-energy electrons lead to the decomposition of SF_6 to produce low-fluoride sulfide SF_x (x = 1 to 5). When no other impurities exist in SF_6, SF_x will recover quickly with the following reaction:

$$\begin{gathered} SF_x + (6 - x)F \rightarrow SF_6,\ x = 1 \sim 5 \\ k = (1.5 \sim 2.4) \times 10^{11} \end{gathered} \tag{7}$$

Here, k is the rate constants of the reaction. However, during the long-term operation of the SF_6 gas-insulated equipment, it is inevitable that different amounts of ultra-impurity gases, such as H_2O and O_2, will appear in the chamber, released by the internal material of the device and the penetration of external H_2O and O_2 into the equipment. The impurities will lead to a series of more complex chemical reactions with SF_x and generate SO_2F_2, SOF_2, HF, SO_2, and other compounds. Therefore, trace amounts of H_2O and O_2 play a key role in the production of SO_2F_2 and SOF_2.

4.1 Analysis of the characteristic decomposed component with the impact of H_2O

H_2O will undergo the following reaction under PD when H_2O exists:

$$e + H_2O \rightarrow H + OH + e \tag{8}$$

$$OH + OH \rightarrow O + H_2O \tag{9}$$

Meanwhile, the following reactions will occur among H_2O and SF_6 decompositions:

$$F + H_2O \rightarrow HF + OH\ ,\ k = 9.0 \times 10^{-12}\ cm^3/s \tag{10}$$

$$F + OH \rightarrow FOH,\ k = 5.0 \times 10^{-13}\ cm^3/s \tag{11}$$

The reaction rate constants k of the reaction (10), (11) and reaction (7), are in the same order of magnitude. On the other hand, the mass action law [14] tells us that the chemical reaction rate r depends on the reactant concentration, C_i, the stoichiometry number, b_i, rate and the constant k, and the relationship is as follows:

$$r = k \prod_i c_i^{b_i} \tag{12}$$

Fortunately, under PD, for all of the chemical reactions where SF_6 and H_2O are involved, the stoichiometry number b_i is one. This finding suggests that the reaction rate r is proportional to the concentration of the reactants. Therefore, when traces of H_2O exist, H_2O has a capture function of F equivalent to the inhibition of the recovery reaction $SF_x + (6\text{-}x)\ F \rightarrow SF_6$. H_2O inhibits the low-fluoride sulfide SF_x (x = 1, 2, 3, 4, 5) composite to SF_6, so that the concentration of SF_4, SF_5, and other components are increased. Additionally, under PD, the trace amount of H_2O has always been small compared with a variety of low-fluoride sulfide SF_x. Thus, the rates of reaction above are mainly determined by the concentration of H_2O. The higher the concentration of H_2O, the more severe the reaction and the more obvious the inhibition, as explained by the following reactions:

$$SF_5 + OH \rightarrow SOF_4 + HF,\ k = 1.1 \times 10^{-12}\ cm^3/s \tag{13}$$

$$SF_5 + O \rightarrow SOF_4 + F,\ k = 2.0 \times 10^{-11}\ cm^3/s \tag{14}$$

$$SOF_4 + H_2O \rightarrow SO_2F_2 + 2HF,\ k = 2.0 \times 10^{-21}\ cm^3/s \tag{15}$$

Formulas (8) to (11) and (13) to (14) show that when SF_6 is mixed with H_2O, H_2O plays a role in providing OH and O. Hence, the formation of SOF_4 is promoted. Meanwhile, reactions (6) to (11) and (13) to (15) constitute a comprehensive reaction, which is the means by which SO_2F_2 is generated. The generation capacity for SO_2F_2 is determined by trot reaction (15), and with the increasing concentration of H_2O, the amount of SO_2F_2 will slightly increase. However, with nearly 10 orders of magnitude of reaction rate in (15) than the rates of reaction in (10), (11), (13), and (14), and with increased concentration of H_2O, the increase of SO_2F_2 is not obvious, as shown in Fig. 4(a).

On the other hand, the reaction between SF_4 and H_2O will occur as follows [8]:

$$SF_4 + H_2O \rightarrow SOF_2 + 2HF\ ,\ k = 1.5 \times 10^{-19}\ cm^3/s \tag{16}$$

The reactions in (16) and (12) show that when the concentration of H_2O increases in SF_6, it will promote the production of SOF_2, as shown in Fig. 4 (b). However, the reaction rate constant k of reaction (16) is 2 orders of magnitude higher than reaction (15). Therefore, with the increased concentration of H_2O in SF_6, the rate of increase of the SOF_2 produced is significantly higher than that of SO_2F_2, as shown in Fig. 4(b).

The effect of H_2O on SF_6 decomposition characteristics under PD can be summarized as follows:

(1) H_2O has a capture function of F which inhibits the low-fluoride sulfide SF_x (x = 1, 2, 3, 4, 5) composite to recombine with SF_6, leading to the increase in the main low-fluoride sulfide SF_5, SF_4, and other components. The higher the concentration of H_2O, the more severe the reaction and the more obvious the inhibition.
(2) H_2O provides OH and O for the generation of oxygen-containing-sulfur-fluoride compounds, and promotes

the generation of the intermediate product SOF_4.

(3) H_2O plays a role in promoting the generation of the final and stable oxygen-containing-sulfur- fluoride compounds, such as SO_2F_2 and SOF_2. However, because the hydrolysis reaction rate of SF_4 is nearly two orders of magnitude higher than SOF_4, the chemical reaction rate r of SF_6 and H_2O under PD is proportional to the concentration of H_2O. Thus, with the growth of the concentration of H_2O in SF_6, the growth rate of SOF_2 is significantly higher than that of SO_2F_2. From the foregoing generalizations, the impact of H_2O on SOF_2 is significantly higher than the impact of SO_2F_2. Thus, the formation of SOF_2 has a positive linear association with the concentration of H_2O.

4.2 Analysis of the impact of O_2 on the characteristic decomposed component

In the case of SF_6 mixed with O_2, under the impact of high-energy electrons produced by PD, in addition to reactions (6) and (7), the following reactions will occur:

$$O_2 + e \rightarrow 2O + e \tag{17}$$

Besides the fact that the free state O generated by reaction (17) will react with SF_5 generated by PD and generate SOF_4, the action below will happen and generate SOF_4:

$$SF_4 + O \rightarrow SOF_4 \tag{18}$$

Then, both SOF_4 and SF_4 react with the H_2O released by the electrodes and the internal wall of the decomposition equipment and generate SO_2F_2, and SOF_2. While O_2 exists, SF_2 will be involved in the following reaction:

$$SF_2 + O_2 \rightarrow SO_2F_2 \tag{19}$$

At present, the reaction rate constant of reaction (19) has not been found yet. Reference [8] has given the maximum rate constant $k=5.0\times10^{-16}$ cm^3/s. Similarly, under PD, the stoichiometric number b_i of reaction (14) and the chemical reactions SF_6 and O_2 are involved in are also equal to one, and O_2 is always a small amount compared with a variety of low-fluoride sulfide SF_x. Thus, the rate of reaction in (19) is proportional to the concentration of O_2. The higher the concentration of O_2, the more severe the reaction and the more SO_2F_2 is generated.

For SO_2F_2, it can be seen from Fig. 5 (a) that when the concentration of O_2 mixed in SF_6 is less than 460ppm, the formation of SO_2F_2 decreases with the increase of O_2. When the concentration of O_2 is higher than 460ppm, the concentration of SO_2F_2 is positively correlated with the concentration of O_2 because an increase in the concentration of O_2 in SF_6 is equivalent to the dilution of SF_2, SF_4, SF_5, and other low-sulfur and fluorine F. Thus, O_2 plays an inhibitory effect on the reaction:

$$SF_x + (6 - x)F \rightarrow SF_6,\ x = 1 \sim 5$$

Although the concentrations of SF_2, SF_4, SF_5, and other low-sulfur components increase with the discharge and promote the reaction in (18) ~ (19), with the increase in the concentration of O_2, the concentration of H_2O released by the electrodes and the internal wall of the decomposition equipment is diluted, making the rate of reactions in (8) to (11) and (15) decrease. Reaction (19) is at lower status when competing with reaction (14), (15) and (18), thus leading to the reduction in the amount of SO_2F_2 generated within 10 hours.

However, when the concentration of O_2 is higher than 460ppm, with a further increase of O_2, the rate of reaction in (18) undergoes a significant increase, and the rates of reaction in (8) to (11) and (15) are no longer significantly reduced. This time, since the concentration of O_2 is high, reaction (19) plays a dominant role in the generation of SO_2F_2 when competing with reaction (14), (15), (18). Thus, when the concentration of O_2 is above 460ppm, the yield of SO_2F_2 increases with the increase of O_2. Hence, with a low concentration of O_2 (the concentration of O_2 < 460 ppm), the dilution of the inherent moisture in the device is the most important factor that affects the formation of SO_2F_2 and the stability of the decomposition under PD. Furthermore, the reactions in (8) to (11) and (15), (18) play leading roles in the formation of SO_2F_2. But at high concentration of O_2 (the concentration of O_2 > 460ppm), reaction (19) plays a leading role in the generation of SO_2F_2, as shown in Fig. 5(a).

For SOF_2, its formation always decreases with the increase of O_2, but the reduction is not obvious when the concentration of O_2 is higher than 460ppm. The reason for the practically unobservable reduction is that with the increase of O_2 mixed in SF_6, SF_2, SF_4, SF_5, and other low-sulfur, fluorine F undergoes a dilution process, thus playing an inhibitory effect on the reaction:

$$SF_x + (6 - x)\,F \rightarrow SF_6,\ \ x = 1 \sim 5$$

Although the concentrations of SF_2, SF_4, SF_5, and other low-sulfur components increase with the discharge, as the concentration of O_2 increases, the concentration of H_2O released by the electrodes and the internal wall of the chamber is diluted at the same time. The rate of the reaction which plays a decisive role in the generation of SOF_2 is shown in the following reaction:

$$SF_4 + H_2O \rightarrow SOF_2 + 2HF,\ \ k = 1.5\times10^{-19}\ cm^3/s$$

will decrease with the decrease in the concentration of H_2O. This phenomenon is most prominent when H_2O is diluted (the concentration of O_2 < 460ppm). With further dilution of H_2O (the concentration of O_2 > 460ppm), the

decrease in the reaction rate is not obvious, resulting in a significant decrease in the formation of SOF_2 with the increase of O_2 when O_2 is at a low concentration. When O_2 is at a high concentration, the decrease in the formation of SOF_2 is not obvious with the increase of O_2, as shown in Fig. 5(b).

In summary, the concentration of H_2O in the reaction chamber decreases because of the dilution effect of O_2, resulting in the reaction rate of a series of reactions in which H_2O decreases and the yield of SOF_2 decreases with the increase of O_2. However, as O_2 promotes the formation of SO_2F_2, at the same time, the formation of SO_2F_2 has a U-shaped relationship curve with the concentration of O_2.

5. Conclusion

(1) Both H_2O and O_2 influence the main characterisitic components SO_2F_2 and SOF_2 during PD, but their by-products and degrees of influence are different. The influence of H_2O on SOF_2 is the most significant and the formation of SOF_2 has a positive linear relationship to the concentration of H_2O while its influence on SO_2F_2 is not obvious. The concentration of O_2 influences the formation of both SO_2F_2 and SOF_2 while the influence is much more obvious on SOF_2.

(2) H_2O has the ability to catch an F atom and to inhibit the low-fluoride sulfide SF_x by recombining to SF_6, which increases the concentration of SF_5 and SF_4. H_2O offers OH and O for the formation of oxygenated-sulfur fluoride, which creates a favorable condition for the ultimate formation of SO_2F_2 and SOF_2. However, the hydrolysis rate of SF_4 is much higher than the hydrolysis rate of SOF_4 (nearly two orders of magnitude higher), as a result, the increase in the rate of SOF_2 is much higher than that of SO_2F_2 when the concentration of H_2O increases.

(3) When the concentration of O_2 is low, the content of H_2O in the equipment is the main factor which influences the fomation of SO_2F_2. When the concentration of O_2 is high, the reaction $SF_2 + O_2 \rightarrow SO_2F_2$ contributes mostly to the fomation of SO_2F_2, Thus, O_2 is the main factor. As for SOF_2, an increase of concentration would diminish the H_2O concentration, in which case O_2 becomes the most important factor in the decrease of SOF_2.

(4) The trace levels of H_2O and O_2 play key roles on the formation of characteristic decomposed components of SF_6 during PD and have significant influence on the products, so it is necessary to study the decomposition mechanism of SF_6 under different concentrations of H_2O and O_2 under the long run PD, and research on different concentrations will help achieve sufficient knowledge on what influences the regularity in the reactions to propose correction methods accordingly. Acquiring sufficient knowledge on the decomposition mechanism and the factors that affect variation in the reactions under PD will lay a solid foundation in using decomposed components of SF_6 to assess insulation status and will support related repair guidelines for gas insulated electrical equipment.

Acknowledgment

The research work has been funded by National Natural Science Foundation of China (Grant No. 51177181), Key Technology R&D Innovation Program of Hubei Province (Grant No. 2014AAA015) and Foundation of State Key Laboratory of Power Transmission Equipment & System Security (Grant No. 2007DA10512714102). The authors sincerely thank the granting agency.

Reference

[1] Sauers, "By-Product Formation in Spark Breakdown of SF_6/O_2 Mixtures," *Plasma Chemistry and Plasma Processing*, vol. 8, no. 2, pp. 247-262, Jun. 1988.

[2] R. J. Van Brunt, "Processes Leading to SF_6 Decomposition in Glow-Type Corona Discharges," *Physics of Ionized Gases*, pp. 161-172, 1989.

[3] R. J. Van Brunt, L. W. Sieck, I. Sauers, and M. C. Siddagangappa, "Transfer of F^- in the Reaction of SF_6^- with SOF_4: Implications for SOF_4 Production in Corona Discharges," *Plasma Chemistry and Plasma Processing*, vol. 8, no. 2, pp. 225-246, Jun. 1988.

[4] C. Pradayrol, A.M. Casanovas, C. Aventin, J. Casanovas, "Production of SO_2F_2, SOF_4, (SOF_2+SF_4), S_2F_{10}, S_2OF_{10} and SO_2F_{10} in SF_6 and (50-50) SF_6-CF_4 Mixtures Exposed to Negative Coronas," *Journal of Physics D-Applied Physics*, vol. 30, no. 9, pp. 1356-1369, May. 1997.

[5] A. M. Casanovas, J. Casanovas, F. Lagarde, and A. Belarbi, "Study of the Decomposition of SF_6 under DC Negative Polarity Corona Discharges (Point-to-Plane Geometry) - Influence of the Metal Constituting the Plane Electrode," *Journal of Applied Physics*, vol. 72, no. 8, pp. 3344-3354, Oct. 1992.

[6] F. Y. Chu, "SF_6 Decomposition in Gas-insulated Equipment," *IEEE Trarnsactions on Electrical Insulatiorn*, vol. 21, no. 5, pp. 693-725, Oct. 1986.

[7] R. J. Van Brunt and J. T. Herron, "Fundamental Processes of SF_6 Decomposition and Oxidation in Glow and Corona Discharges," *IEEE Transactions on Electrical Insulation*, vol. 25, pp. 75-94, Feb. 1990.

[8] R. J. Van Brunt and J. T. Herron, "Plasma Chemical-Model for Decomposition of SF_6 in a Negative Glow Corona Discharge," *Physica Scripta*, vol. T53, pp. 9-29, 1994.

[9] Ju Tang, Fuping Zeng, Jianyu Pan, et al. "Correlation

Analysis Between Formation Process of SF_6 Decomposed Components and Partial Discharge Qualities," *IEEE Transactions on Dielectrics and Electrical Insulation*, vol. 20, pp. 864-875, 2013.

[10] Fuping Zeng, Ju Tang, Qingtao Fan, Jianyu Pan, Xiaoxing Zhang et al. Decomposition Characteristics of SF_6 under Thermal Fault for Temperature below 400℃[J]. *IEEE Transactions on Dielectrics and Electrical Insulation*, Vol. 21, No. 3, pp: 995-1004, 2014

[11] Ju Tang, Fuping Zeng, Xiaoxing Zhang, Jianyu Pan et al. Relationship between Decomposition Gas Ratios and Partial Discharge Energy in GIS, and the Influence of Residual Water and Oxygen[J]. *IEEE Transactions on Dielectrics and Electrical Insulation*, Vol. 21, No. 3, pp: 1226-1234, 2014

[12] IEC60480-2004, "Guidelines for the checking and treatment of sulfur hexafluoride (SF_6) taken from electrical equipment and specification for its re-use," 2004.

[13] R. J. Van Brunt and M. C. Siddagangappa, "Identification of Corona Discharge-Induced SF_6 Oxidation Mechanisms Using $SF_6/(^{18}O_2)/(H_2{}^{16}O)$ and $SF_6/(^{16}O_2)/(H_2{}^{18}O)$ Gas-Mixtures", Plasma Chemistry and Plasma Processing, vol. 8, no. 2, pp. 207-223, Jun. 1988.

[14] James H. Espenson, "Chemical Kinetics and Reaction Mechanism," McGraw-Hill Press, Inc., New York, Ch.2, pp. 39-56, 1995.

[15] A. Derdouri, J. Casanovas, R. Hergli, R. Grob, and J. Mathieu, "Study of the Decomposition of Wet SF_6, Subjected to 50-Hz AC Corona Discharges," *Journal of Applied Physics*, vol. 65, no. 5, pp. 1852-1857, Mar. 1989.

[16] Tang Ju, Liu Fan, "Partial Discharge Recognition by Analysis of SF6 Decomposition Products Part 1: Decomposition Characteristic of SF_6 under Four Different Partial Discharges," *IEEE Trans. Dielectrics and Electrical Insulation*, vol. 19, no. 1, pp. 29-36, Feb. 2012.

[17] A. M. Casanovas, I. Coll, and J. Casanovas, "Decomposition Products From Negative and 50 Hz AC Corona Discharges in Compressed SF_6 and SF_6/N_2 (10:90) Mixtures. Effect of Water Vapour Added to the Gas," *Journal of Physics D-Applied Physics*, vol. 32, no. 14, pp. 1681-1692, Jul. 1999.

[18] W. Tsang and J. T. Herron, "Kinetics and Thermodynamics of the Recation SF_6 Reversible SF_5 + F," *Journal of Chemical Physics*, vol. 96, no. 6, pp. 4272-4282, Mar. 1992.

[19] J. Shao, "Mathematical statistics," World Publishing, Co., Ch.6, pp. 81-93, 2009.

Fuping Zeng was born in Chongqing, China in 1984. He obtained his bachelor's degree in electrical engineering from Dalian Maritime University, and his master's and doctoral degrees from the State Key Laboratory of Power Transmission Equipment & System Security and New Technology, Chongqing University, China. He is currently a postdoctoral research at the School of Electrical Engineering, Wuhan University, China. He is involved in the online monitoring and fault diagnosis of high-voltage electric equipment insulation. E-mail: Fuping.Zeng@whu.edu.cn

Ju Tang was born in Pengxi, Si Chuan Province, China in 1960. He obtained his bachelor's degree from Xi'an Jiaotong University, and his master's and doctoral degrees from Chongqing University. Dr. Tang is a professor at the State Key Laboratory of Power Transmission Equipment and System Security and New Technology, Chongqing University; a professor at the School of Electrical Engineering in Wuhan University, China; and the chief scientist presiding over the National Basic Research Program of China (973 Program) (2009CB724500). He is currently involved in the online monitoring and fault diagnosis of high-voltage electric equipment insulation.

Yanbin Xie was born in Chongqing, China, in 1980. He received the Bachel / Master and doctoral degrees in electrical engineering from Chongqing University, China. He is now working in State Grid Chongqing Electric Power Company, Shiqu Power Supply Company, China, and he is involved in online highvoltage detection equipment and signal processing. E-mail:yanbinse @126.com

Qian Zhou was born in Kaifeng, Henan Province, China, in 1980. She received the Bachel/Master and doctoral degrees in electrical engineering from Chongqing University, China. She is now working in State Grid Chongqing Electric Power Company, China, and she is involved in on-line high-voltage detection equipment and signal processing. E-mail: cquzhou@163.com

Chaohai Zhang was born in Harbin, Heilongjiang Province, China in 1966. He obtained his bachelor's degree from Harbin Institute of Technology, his master's from Naval University of Engineering, and his doctoral degrees from Hong Kong Polytechnic University. Dr. Zhang is now working in Wuhan NARI Limited Company of State Grid Electric Power Research Institute, China. He is currently involved in the online monitoring and fault diagnosis of high-voltage electric equipment insulation.